

**[AMT01] Synthesis and characterisation of new bismuth phosphate sillenite materials****Lee Siew Ling<sup>1</sup>, Lee Chnoong Kheng<sup>1</sup> and Derek C. Sinclair<sup>2</sup>**<sup>1</sup>Department of Chemistry, Faculty of Science and Environmental Studies, Universiti Putra Malaysia, 43400 Serdang, Selangor, Malaysia.<sup>2</sup>Department of Engineering Materials, University of Sheffield, Sheffield S1 3JD, UK.**Introduction**

Sillenite compounds,  $\text{Bi}_{12}\text{MO}_{20}$ , where M = Ge, Si, Ti, P, Pb, B (Lobato *et al.*, 2000; Valent and Suvorov, 2001; Valent and Suvorov, 2002; Wignacourt *et al.*, 1991; Marinova *et al.*, 2002) have been studied for their electro-optical, photoconductivity and dielectric properties. The general formula for stoichiometric sillenites is  $\text{Bi}_{12}\text{MO}_{20}$  where M represents a tetravalent element occupying B-site in the crystal structure that belongs to the *I23* space group with a body-centred cubic cell (Swindells and Gonzalez, 1988; Horowitz *et al.*, 1989). Several different mechanisms of isomorphic substitution allow the formation of defective sillenites with cation and oxygen vacancies and possibly even oxygen excess (Swindells and Gonzalez, 1988). There have been some controversies regarding the occupancy of the tetrahedral M site in the sillenite structure. In the study of the structure of  $\text{Bi}_{25}\text{FeO}_{40}$  and  $\text{Bi}_{38}\text{ZnO}_{60}$  sillenites by X-ray method (Craig and Stephenson, 1975), the authors suggested that the M-cation valence or effective valence of the isomorphous cationic mixture at the M site was always equal to four. Thus the Bi atom partially occupying the M-site was pentavalent and the compositions corresponded to  $\text{Bi}_{24}^{3+}\text{Bi}^{5+}\text{Fe}^{3+}\text{O}_{40}$  and  $\text{Bi}_{36}^{3+}\text{Bi}_2^{5+}\text{Zn}^{2+}\text{O}_{60}$ , respectively. Similarly the structure of body-centred cubic  $\gamma\text{-Bi}_2\text{O}_3$  was proposed to be  $\text{Bi}_{25}^{3+}\text{Bi}^{5+}\text{O}_{40}$ . Watanabe *et al.* (1990) stated that full occupancy of the tetrahedral site was the first necessity to the stability of the sillenite-type structure and suggested that a bismuth phosphate sillenite-type material containing 6.73 mol%  $\text{P}_2\text{O}_5$  had the composition  $\text{Bi}(\text{III})_{23.33}[\text{Bi}(\text{V})_{0.295}\text{P}_{1.705}]\text{O}_{40}$  while  $\gamma\text{-Bi}_2\text{O}_3$  would be  $\text{Bi}(\text{III})_{23.33}\text{Bi}(\text{V})_2\text{O}_{40}$ . There was, however, no experimental evidence to support the existence of Bi(V). Radaev *et al.* (1991), on the other hand, proposed that the

compositions for sillenite compounds where M = (Bi, Fe) and (Bi, Zn) were  $\text{Bi}_{12}(\text{Bi}_{0.5}^{3+}\text{Fe}_{0.5}^{3+})\text{O}_{19.50}$  and  $\text{Bi}_{12}(\text{Bi}_{0.67}^{3+}\text{Zn}_{0.33}^{2+})\text{O}_{19.33}$ , respectively based on neutron diffraction data. They proposed a new model for  $\gamma\text{-Bi}_2\text{O}_3$  which was represented as  $\text{Bi}_{12}\text{Bi}_{0.8}\text{O}_{19.20}$  or  $\text{Bi}_{12}[\text{BiO}_3]_{0.8}[\text{O}_4]_{0.2}\text{O}_{16}$ , *i.e.* with 80% occupancy of tetrahedral site by  $\text{Bi}^{3+}$  in the form of umbrella like  $[\text{BiO}_3]$  groups and void tetrahedra (Radaev *et al.*, 1992).

In a neutron powder diffraction study of  $\text{Bi}_{12}\text{PbO}_{19}$  it was shown that at low and room temperature a sillenite structure was adopted in which the anion vacancies were localized to specific locations on the sublattice (Murray *et al.*, 1986). A fluorite structure related to the  $\delta\text{-Bi}_2\text{O}_3$  and an ionic conduction was observed in this material at higher temperature.

The existence of defective crystal structures suggests potentially interesting and intriguing electrical properties in these materials. Here we report the synthesis and characterisation of sillenite materials in the  $\text{Bi}_2\text{O}_3\text{-P}_2\text{O}_5$  binary system. In addition the formation of solid solutions by isomorphic substitution and their properties are presented.

**Materials and methods**

Bismuth phosphate materials were prepared using  $\text{Bi}_2\text{O}_3$  (99.9%, Aldrich) and  $\text{NH}_4\text{H}_2\text{PO}_4$  (99%, Merck) as reagents via solid state reactions. The reagents used in the study of chemical doping included  $\text{As}_2\text{O}_5$  (99.9%, Alfa Aesar),  $\text{V}_2\text{O}_5$  (99.8%, Ventron),  $\text{PbO}$  (99.9%, Alfa Aesar),  $\text{Sr}(\text{NO}_3)_2$  (99.97%, Alfa Aesar),  $\text{Al}_2\text{O}_3$  (99.5+%, Fluka),  $\text{Ga}_2\text{O}_3$  (99.999%, Alfa Aesar),  $\text{Fe}_2\text{O}_3$  (99.99%, Johnson Matthey Electronics),  $\text{SiO}_2$  (99.995%, Alfa Aesar),  $\text{GeO}_2$  (99.9999%, Johnson Matthey Electronics) and  $\text{TiO}_2$  (99.99%, Aldrich). All the oxides except  $\text{As}_2\text{O}_5$  were dried at 300°C prior to weighing.  $\text{As}_2\text{O}_5$  was dried at 200°C while  $\text{NH}_4\text{H}_2\text{PO}_4$  and

Sr(NO<sub>3</sub>)<sub>2</sub> were used as supplied. Compositions were weighed (*ca.* 3g total), mixed with acetone in an agate mortar, dried and fired in Au foil boats at temperatures in the range of 750°C to 820°C and duration of 2-10 days, with intermediate regrinding. Weight-loss checks on these samples showed that material loss through volatilisation was not significant.

The samples were analysed by X-ray powder diffraction (Shimadzu diffractometer XRD 6000, CuK<sub>α</sub> radiation). Electrical properties were determined by ac impedance spectroscopy using a Hewlett-Packard Impedance Analyzer HP 4192A in the frequency range of 10 Hz to 13 MHz. Pellets were cold pressed and sintered at 750-820°C overnight; Au paste electrodes were then fired on at 200-600°C. Measurements were made between 300°C and 820°C by incremental steps of 50°C (or 10°C for temperature ranges 650°C < T < 820°C) with 30 min equilibration time. Most measurements were made in air, and where necessary in nitrogen.

For differential thermal analysis (DTA) and thermogravimetric analysis (TGA), a Perkin-Elmer instrument (model DTA 7 and TGA 7) with a heating and cooling rate of 10°C min<sup>-1</sup> was used.

## Results and discussion

### Phase formation and purity

Compositions ranging from Bi:P of 10:1 to 25:1 in the Bi<sub>2</sub>O<sub>3</sub>-P<sub>2</sub>O<sub>5</sub> binary system were synthesised and results are shown in Table 1.

Mixed phases of Bi<sub>7</sub>PO<sub>13</sub> (monoclinic symmetry with space group of *P2<sub>1</sub>*), a cubic phase with space group *Fm3m* and sillenite phase with space group *I23* were formed for materials with Bi:P ratios of 10:1 and 11:1 prepared at 800°C for 48 hours. For the composition of 12:1, the mixture consisted of Bi<sub>7</sub>PO<sub>13</sub> and sillenite phase. When a small amount of the melted sample (~0.3 g) was quenched in Hg the XRD pattern was that of single-phase cubic form, space group *Fm3m*.

TABLE 1 Phase assemblage in *x*Bi<sub>2</sub>O<sub>3</sub>-P<sub>2</sub>O<sub>5</sub> binary system, 10 ≤ *x* ≤ 25.

Bi:P ratio	Heat treatment	Phases
10:1	800°C, 48 h melted and Hg quenched	Sillenite, Bi <sub>7</sub> PO <sub>13</sub> and cubic phase, <i>Fm3m</i> Cubic phase, <i>Fm3m</i> , a = 5.5131 Å
11:1	800°C, 48 h melted and Hg quenched	Sillenite, Bi <sub>7</sub> PO <sub>13</sub> and cubic phase, <i>Fm3m</i> Cubic phase, <i>Fm3m</i> , a = 5.5128 Å
12:1	800°C, 48 h melted and Hg quenched	Sillenite and Bi <sub>7</sub> PO <sub>13</sub> Cubic phase, <i>Fm3m</i> , a = 5.5307 Å
13:1	750°C, 48 h melted and Hg quenched	Sillenite Cubic phase, <i>Fm3m</i> , a = 5.5272 Å
14:1	800°C, 48 h	Sillenite
15:1	750°C, 48 h	Sillenite
16:1	800°C, 60 h, Hg quenched	Sillenite
17:1	800°C, 60 h, Hg quenched	Sillenite and γ-Bi <sub>2</sub> O <sub>3</sub>
18:1	800°C, 60 h, Hg quenched	Sillenite and γ-Bi <sub>2</sub> O <sub>3</sub>
19:1	800°C, 60 h, Hg quenched	Sillenite and γ-Bi <sub>2</sub> O <sub>3</sub>
20:1	800°C, 60 h, Hg quenched	Sillenite, γ-Bi <sub>2</sub> O <sub>3</sub> and Bi <sub>2</sub> O <sub>3</sub> <sup>a</sup>
22:1	800°C, 60 h, Hg quenched	Sillenite, γ-Bi <sub>2</sub> O <sub>3</sub> and Bi <sub>2</sub> O <sub>3</sub> <sup>a</sup>
25:1	800°C, 12 h, Hg quenched melted and Hg quenched	Sillenite, Bi <sub>2</sub> O <sub>3</sub> <sup>a</sup> and an unidentified phase Tetragonal phase, a = 5.5307 Å, c = 5.6469 Å

<sup>a</sup> Bismite, syn, monoclinic, ICDD card no: 41-1449.

Single phase sillenite compounds were formed for materials with Bi:P ratios of 13:1 to 16:1. The XRD patterns of these materials could be fully indexed using Chekcell refinement software and the cell parameters are listed in Table 2. Lattice parameters and volumes of these materials increased with increase of Bi

content. The ionic radius of  $\text{Bi}^{3+}$  (0.96 Å) is larger than  $\text{P}^{5+}$  (0.17 Å) (Shannon and Prewitt, 1969). It was thus expected that substitution of Bi into P site would result in an increase of the cell constant.  $\text{Bi}_{14}\text{PO}_8$  prepared by manual mixing has a larger cell parameter than that prepared by ball milling.

TABLE 2 Lattice parameter and cell volume of sillenite-type phases as a function of Bi/P ratio from X-ray diffraction data

Sample	Cell parameters	Cell parameters reported/ reference
$\text{Bi}_{13}\text{PO}_8$	cubic, <i>I23</i> a = 10.1660(4) Å V = 1050.6 Å <sup>3</sup>	cubic, <i>I23</i> a = 10.169(1) Å (ICDD card no: 81-443)
$\text{Bi}_{14}\text{PO}_8$	cubic, <i>I23</i> a = 10.1681(1) Å V = 1051.28 Å <sup>3</sup>	cubic, <i>I23</i> a = 10.1761(4) Å V = 1053.77 Å <sup>3</sup> (Bi:P=13.953:1, ICDD card no: 44-199)
$\text{Bi}_{15}\text{PO}_8$	cubic, <i>I23</i> a = 10.1733 (3) Å V = 1052.89 Å <sup>3</sup>	
$\text{Bi}_{16}\text{PO}_8$	cubic, <i>I23</i> a = 10.1765 (1) Å V = 1053.89 Å <sup>3</sup>	

At higher Bi:P ratios, a mixture of sillenite phase and  $\gamma\text{-Bi}_2\text{O}_3$  were obtained. Usually,  $\gamma\text{-Bi}_2\text{O}_3$  was formed at  $\sim 640^\circ\text{C}$ , and it persisted to room temperature when cooling rate was kept very low (Sammes *et al.*, 1999). Therefore, it was possible to eliminate traces for  $\gamma\text{-Bi}_2\text{O}_3$  at compositions with Bi:P ratio of 16:1 by quenching the material in Hg. The crystal structure of  $\gamma\text{-Bi}_2\text{O}_3$  has, in fact, be described as a defective sillenite with formula  $\text{Bi}_{12}\text{Bi}_{0.80}\text{O}_{19.20}$  (Radeav *et al.*, 1992). Wignacourt *et al.* (1991, 1991b) reported the formation of single-phase  $\gamma$  solid solutions with a sillenite type unit cell for compositions with Bi:P ratios of 13:1 to 19:1. In the present study, however, it was not possible to eliminate  $\gamma\text{-Bi}_2\text{O}_3$  at Bi:P ratios higher than 16:1.

The material of composition Bi:P = 14:1 was selected for characterisation and further studies. Assuming that all the Bi exists as Bi(III) the formula of this material could be written as  $\text{Bi}_{12}\text{P}_{0.857}\text{O}_{20.14}$  with partial occupation of tetrahedral site and slight excess of oxygen. On the other hand, if Bi exists as both Bi(III) and Bi(V) and there is full occupancy of the tetrahedral site as suggested by Watanabe *et al.* (1990) the formula would be  $\text{Bi}_{11.825}\text{P}_{0.845}\text{O}_{20}$  or  $\text{Bi(III)}_{11.67}[\text{Bi(V)}_{0.155}\text{P}_{0.845}]\text{O}_{20}$  with 2.78% vacancy on Bi(III) site. The exact formula of this material can only be confirmed with crystallographic structure determination. For ease of description and comparison we would present the material as having composition  $\text{Bi}_{14}\text{PO}_8$  in this paper.

#### Thermal analysis

DTA was carried out on single phase materials with a heating and cooling rate of  $10^\circ\text{C}/\text{min}$  in the temperature range of  $35^\circ\text{C}$  to  $860^\circ\text{C}$ . All the materials exhibit similar DTA results.

Figure 1 shows the DTA curves of two heat-cool cycles for  $\text{Bi}_{14}\text{PO}_8$ . In the first heating cycle two endothermic peaks were observed at  $829^\circ\text{C}$  and  $850^\circ\text{C}$ , followed by the onset of melting; the cooling cycle shows three exothermic peaks at  $832$ ,  $771$  and  $630^\circ\text{C}$ , respectively. The peak that appeared as a shoulder at  $839^\circ\text{C}$  corresponds to recrystallisation after melting at  $\sim 880^\circ\text{C}$ . An endothermic peak at  $\sim 733^\circ\text{C}$ , which was absent in first heating process was observed in second heating process. Besides, the two endothermic peaks at  $\sim 830^\circ\text{C}$  and  $\sim 850^\circ\text{C}$  were well separated in the second heating process. These phenomena suggest that there were three reversible phase transitions. It has been reported that two polymorphic transitions were observed for sillenite materials of compositions 13:1 to 19:1 at  $820$  and  $867^\circ\text{C}$ , corresponding to  $\gamma \rightarrow \delta'$  and  $\delta' \rightarrow \delta$  transformations, respectively (Wignacourt *et al.*, 1991b). Both  $\delta'$  and  $\delta$  have fluorite type structures. The phase transitions observed at  $819^\circ\text{C}$  and  $848^\circ\text{C}$  probably correspond to the transformations reported earlier.

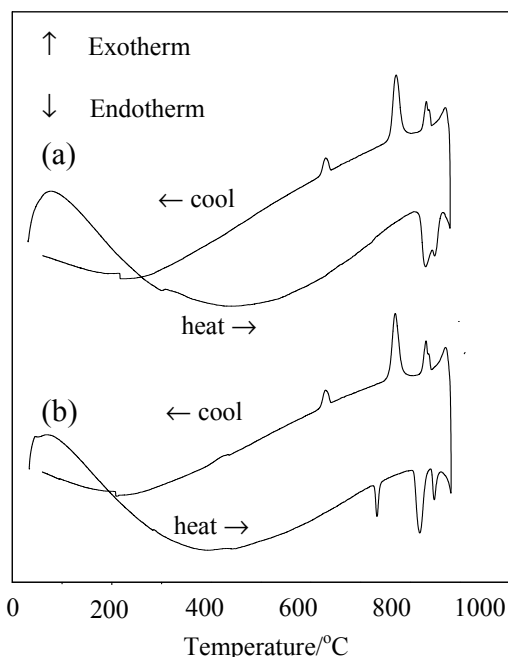


FIGURE 1 DTA thermograms of  $\text{Bi}_{14}\text{PO}_8$  of (a) first cycle and (b) second cycle.

TGA experiments did not reveal any significant weight loss over the range 35-860°C and therefore significant composition changes associated with volatilization of Bi and or P below 860°C can be eliminated.

*Electrical properties*

Conductivity measurements were carried out on single phase materials in the  $x\text{Bi}_2\text{O}_3\text{-P}_2\text{O}_5$  binary system,  $13 \leq x \leq 16$ . Conductivity values of the materials were extracted from impedance complex plane plots. Typical impedance data are shown in Fig 2 for  $\text{Bi}_{14}\text{PO}_8$ . At 400°C, the predominant feature is a single semicircle distorted at low frequency indicating the contribution of grain boundary effect (Figure 2a). The semicircle has an associated capacitance of  $5.6 \times 10^{-12} \text{ F cm}^{-1}$ , which is typical of a bulk component. At higher temperatures, a low-frequency spike inclined at  $\approx 50^\circ$  to the horizontal axis can be clearly seen (Figure 2b). Its associated capacitance of  $\sim 10^{-7} \text{ F cm}^{-1}$  is characteristic of ionic polarization phenomenon at blocking electrodes. At 800°C the spike collapsed to form a semi-circular arc (Figure 2c) indicating that oxygen diffusion was

through a layer of finite thickness (Irvine *et al.*, 1990). It thus appears that the conducting species are predominantly oxide ions.

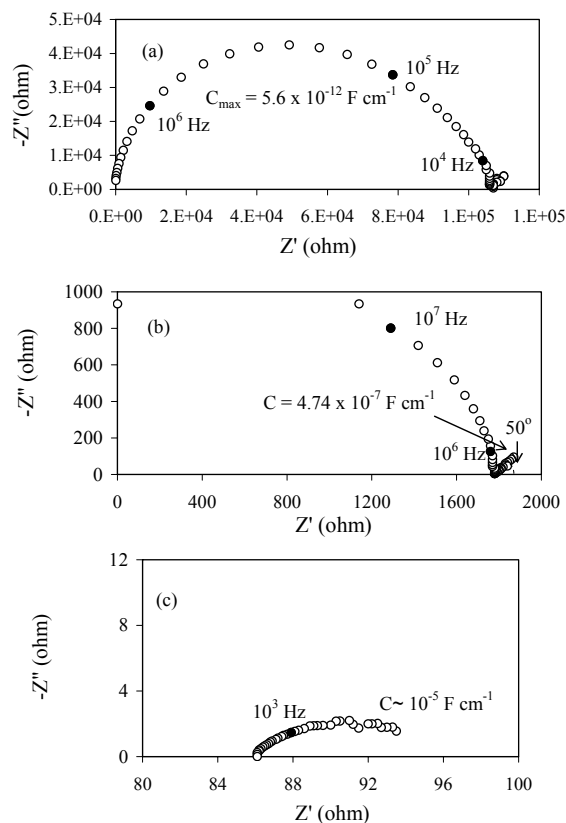
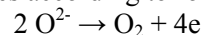


FIGURE 2  $Z^*$  plot of  $\text{Bi}_{14}\text{PO}_8$  at (a) 400°C, (b) 600°C and (c) 800°C.

In order to further examine the conduction species in the materials, conductivity measurements were carried out in dry oxygen free nitrogen (OFN). Isothermal conductivity plots for the sample in OFN and air are given in Figure 3 and show the conductivity to be higher in OFN, indicating that there is electronic contribute to the conduction. At low oxygen partial pressure, oxygen was removed from the sample surface which leads to the generation of n-type carries according to following equation:



The material,  $\text{Bi}_{14}\text{PO}_8$ , thus appears to be a mixed conductor. Wignacourt *et al.* (1991) reported that the electrical conductivity of  $\text{Bi}_{9.872}^{3+} \text{Bi}_{1.223}^{5+} \text{P}_{0.853} \text{O}_{20}$  (Bi:P = 13:1) was typical

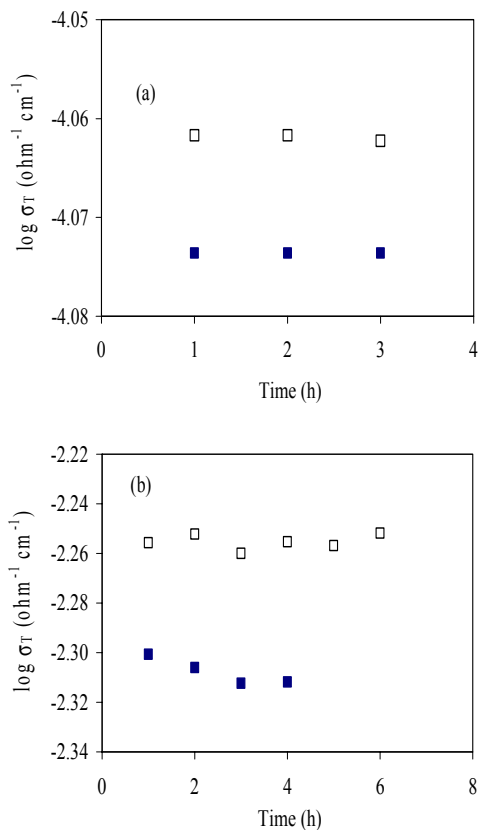


FIGURE 3 Isothermal conductivity of  $\text{Bi}_{14}\text{PO}_8$  in air and nitrogen at (a)  $500^\circ\text{C}$ , (b)  $750^\circ\text{C}$  ( $\square$ ) nitrogen, ( $\blacksquare$ ) air.

of a mixed conduction up to  $820^\circ\text{C}$ . The oxide ion transference number was less than 0.5 at  $400^\circ\text{C} < T < 800^\circ\text{C}$ , but close to unity at  $820^\circ\text{C}$  where phase transformation took place.

Conductivity of the materials in the  $\text{Bi}_2\text{O}_3\text{-P}_2\text{O}_5$  binary system decreases in the order of  $\text{Bi}_{13}\text{PO}_8 \approx \text{Bi}_{14}\text{PO}_8 > \text{Bi}_{15}\text{PO}_8 > \text{Bi}_{16}\text{PO}_8$  (Figure 4). The Arrhenius plots are linear up to  $700^\circ\text{C}$ , with curvature being seen at around  $750^\circ\text{C}$ , corresponding to the  $\gamma \rightarrow \delta'$  phase transition (Wignacourt *et al.*, 1991b). The activation energy which is higher above  $750^\circ\text{C}$  relates to that of migration of oxide ions.

#### Formation of solid solutions and their properties

A complete solid solution series with sillenite structure was obtained when As was introduced to replace P while substitution of P

by V results in the formation of partial solid solutions,  $\text{Bi}_{14}\text{P}_{1-x}\text{V}_x\text{O}_8$ ,  $0 \leq x \leq 0.3$ . Substitution of P by Pb, Sr, Al, Si, Ge, Ti, Ga and Fe resulted in the formation of limited solid solutions, with  $x$  ranging from 0.2 ( $M = \text{Sr}, \text{Pb}$ ) to 0.4 ( $M = \text{Fe}, \text{Ga}$ ) at the solid solution limit in the formula  $\text{Bi}_{14}\text{P}_{1-x}\text{M}_x\text{O}_8$ . Existence of  $\gamma\text{-Bi}_2\text{O}_3$  was observed at higher dopant concentration in these materials.

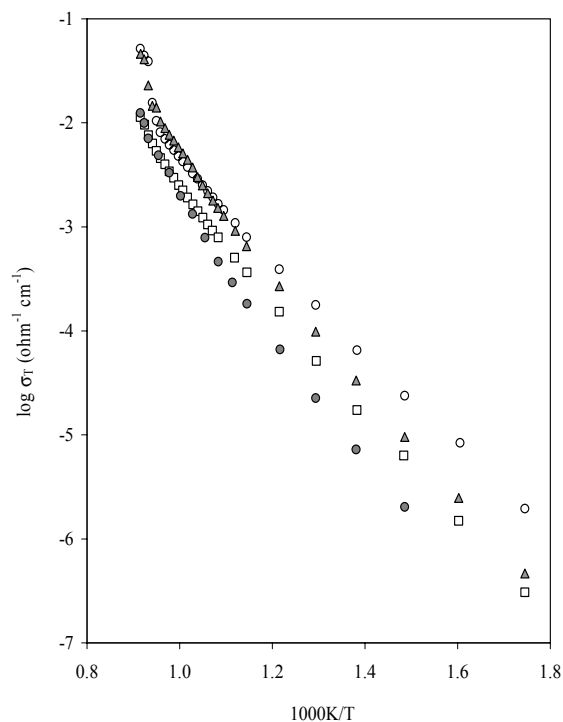


FIGURE 4 Arrhenius plots of conductivity for  $x\text{Bi}_2\text{O}_3\text{-P}_2\text{O}_5$  sillenite materials. ( $\circ$ )  $x = 13$ , ( $\blacktriangle$ )  $x = 14$ , ( $\square$ )  $x = 15$ , ( $\bullet$ )  $x = 16$ .

The DTA results and the complex plane plots of the materials in  $\text{Bi}_{14}\text{P}_{1-x}\text{M}_x\text{O}_8$  solid solutions are similar to that observed in  $\text{Bi}_{14}\text{PO}_8$ .

In  $\text{Bi}_{14}\text{P}_{1-x}\text{As}_x\text{O}_8$  solid solutions, introduction of As into P site in  $\text{Bi}_{14}\text{PO}_8$  did not result in significant changes in the conductivity of the materials. On the other hand, substitution of P by V in  $\text{Bi}_{14}\text{P}_{1-x}\text{V}_x\text{O}_8$  solid solutions led to an enhancement in conductivity. Figure 5 shows the Arrhenius plots of  $\text{Bi}_{14}\text{PO}_8$  and selected doped materials. Enhancement in conductivity was observed only in 5% Pb-, 5%

Si- and 5% Ge-doped materials. However, increasing the dopant concentration to 10% resulted in a decrease in conductivity.

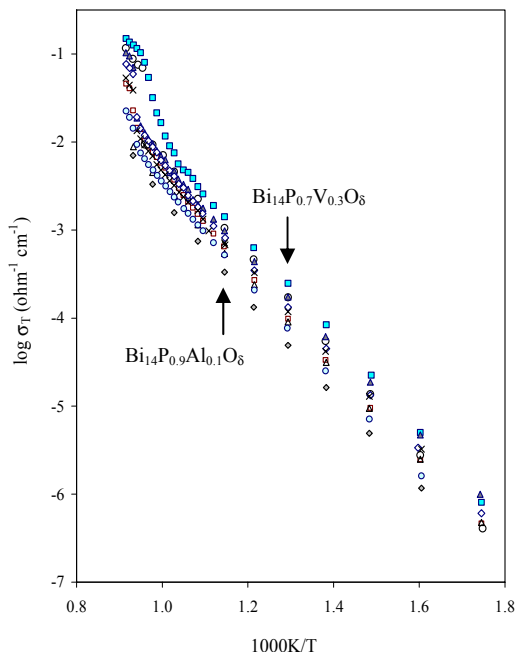


FIGURE 5 Arrhenius plots of  $\text{Bi}_{14}\text{PO}_8$  and some doped materials.

(□)  $\text{Bi}_{14}\text{PO}_8$ ; (○)  $\text{Bi}_{14}\text{AsO}_8$ ; (■)  $\text{Bi}_{14}\text{P}_{0.7}\text{V}_{0.3}\text{O}_8$ ;  
 (▲)  $\text{Bi}_{14}\text{P}_{0.95}\text{Pb}_{0.05}\text{O}_8$ ; (◇)  $\text{Bi}_{14}\text{P}_{0.95}\text{Si}_{0.05}\text{O}_8$ ;  
 (×)  $\text{Bi}_{14}\text{P}_{0.95}\text{Ge}_{0.05}\text{O}_8$ ; (Δ)  $\text{Bi}_{14}\text{P}_{0.95}\text{Ga}_{0.05}\text{O}_8$ ;  
 (●)  $\text{Bi}_{14}\text{P}_{0.95}\text{Fe}_{0.05}\text{O}_8$ ; (◆)  $\text{Bi}_{14}\text{P}_{0.9}\text{Al}_{0.1}\text{O}_8$

In general, conductivity decreases in the order of  $\text{Bi}_{14}\text{P}_{1-x}\text{V}_x\text{O}_8 > \text{Bi}_{14}\text{P}_{1-x}\text{Pb}_x\text{O}_8 > \text{Bi}_{14}\text{P}_{1-x}\text{As}_x\text{O}_8 > \text{Bi}_{14}\text{PO}_8$ . The highest conductivity was obtained in V-doped materials with  $\sigma \sim 27 \text{ mS cm}^{-1}$  (or  $1.27 \times 10^{-1} \text{ ohm}^{-1} \text{ cm}^{-1}$ ) at  $800^\circ\text{C}$  for  $\text{Bi}_{14}\text{P}_{0.3}\text{V}_{0.7}\text{O}_8$ , which is higher than that of yttria stabilised zirconia (YSZ) at the same temperature. The activation energy of  $\sim 0.92 \text{ eV}$  is comparable to that of YSZ. The enhanced conductivity in this composition is due to a reduction in the phase transition temperature from a sillenite-type structure (space group  $I23$ ) to a defect fluorite-type structure related to  $\delta\text{-Bi}_2\text{O}_3$ .

### Conclusion

Sillenite solid solutions were formed in  $\text{Bi}_2\text{O}_3\text{-P}_2\text{O}_5$  binary system and when P was

replaced by V, As and several other elements including Si, Ge, and Pb. In general, these materials exhibit similar conductivity behaviour, *i.e.* they are mixed conductors at temperatures  $< 750^\circ\text{C}$  but undergo polymorphic phase transitions at high temperatures,  $> 800^\circ\text{C}$ , presumably to defect-fluorite-type materials; however, high temperature in situ diffraction studies are required to confirm the crystallography of the high temperature polymorphs. Based on the “stoichiometric” model for sillenites suggested by Valent and Suvorov (2002), the solid solution limit for  $\text{P}^{5+}$  in  $\gamma\text{-Bi}_2\text{O}_3$  would be Bi/P=15:1. Clearly, our data show that the single-phase sillenites can be formed for 16:1 and 15:1, in agreement with this model; however, both our data and that reported by Wignacourt *et al.* (1991) suggest that compositions with Bi/P=14:1 and 13:1 can also be prepared as single-phase sillenite-type materials. It would appear, therefore, that the stoichiometry of several sillenite-type phases remains a complex issue and is worthy of further study.

### Acknowledgement

SLL and CKL are grateful to the Ministry of Science, Technology and Environment for financial support (NSF and IRPA Grant number 09-02-04-0302-EA001, respectively).

### References

- Craig, D.C., Stephenson, N.C. 1975. Structural studies of some body-centered cubic phases of mixed oxides involving  $\text{Bi}_2\text{O}_3$ : the structures of  $\text{Bi}_{25}\text{FeO}_{40}$  and  $\text{Bi}_{38}\text{ZnO}_{60}$ . *J. Solid State Chem.* 15: 1-8.
- Horowitz, H.S., Jacobson, A.J., Newsam, J.M., Lewandowski, J.T. and Leonowicz, M.E. 1989. Solution synthesis and characterization of sillenite phases,  $\text{Bi}_{24}\text{M}_2\text{O}_{40}$  (M = Si, Ge, V, As, P). *Solid State Ionics*, 32/33: 678-690.
- Irvine, J.T.S., Sinclair, D.C., and West, A.R. 1990. Electroceramics: characterization by impedance spectroscopy. *Adv. Mat.* 2(3): 132-138.

- Lobato, A.R., Lanfredi, S., Carvalho, J.F. and Hernandez, A.C. 2000. Synthesis, crystal growth and characterization of  $\gamma$ -phase bismuth titanium oxide with gallium. *Mat. Res.* 3: 92-96.
- Marinova, V., Sainov, V., Lin, S.H., Hsu, K.Y. 2002. DC and AC conductivity measurements of  $\text{Bi}_{12}\text{TiO}_{20}$  photorefractive crystals doped with Ag, P, Cu, Cd. *Jpn. J. Appl. Phys.* 41 (1-3B): 1860-1863.
- Murray, A.D., Catlow, R.A., Beech, F., and Drennan, J. 1986. A neutron powder diffraction study of the low- and high-temperature structures of  $\text{Bi}_{12}\text{PbO}_{19}$ . *J. Solid State Chem.* 62: 290-296.
- Radaev, S.F., Muradyan, L.A. and Simonov, V.I. 1991. Atomic structure and crystal chemistry of sillenites:  $\text{Bi}_{12}(\text{Bi}^{3+}_{0.50}\text{Fe}^{3+}_{0.50})\text{O}_{19.50}$  and  $\text{Bi}_{12}(\text{Bi}^{3+}_{0.67}\text{Zn}^{2+}_{0.33})\text{O}_{19.33}$ . *Acta Cryst.* B47: 1-6.
- Radaev, S.F., Simonov, V.I. and Kargin, Yu.F. 1992. Structural features of  $\gamma$ -phase  $\text{Bi}_2\text{O}_3$  and its place in the sillenite family. *Acta Cryst.* B48: 604-609.
- Sammes, N.M., Thompsett, G.A., Näfe, H., and Aldinger, F. 1999. Review: Bismuth based oxide electrolytes - structure and ion conductivity. *J. European Ceramic Society.* 19: 1801-1826.
- Shannon, R.D. and Prewitt, C.T. 1969. Effective ionic radii in oxides and fluorites. *Acta Cryst.* B25, 925-946.
- Swindells, D.C.N. and Gonzalez, J.L. 1988. Absolute configuration and optical activity of laevorotatory  $\text{Bi}_{12}\text{TiO}_{20}$ . *Acta Cryst.* B44: 12-15.
- Valant, M. and Suvorov, D. 2001. Processing and dielectric properties of sillenite compounds  $\text{Bi}_{12}\text{MO}_{20-\delta}$  (M = Si, Ge, Ti, Pb, Mn,  $\text{B}_{1/2}\text{P}_{1/2}$ ). *J. Am. Ceram. Soc.* 84(12): 2900-2904.
- Valent, M. and Suvorov, D. 2002. Synthesis and characterization of a new sillenite compound -  $\text{Bi}_{12}(\text{B}_{0.5}\text{P}_{0.5})\text{O}_{20}$ . *J. Am. Ceram. Soc.* 85(2): 355-358.
- Watanabe, A., Kodoma H. and Takenouchi, S. 1990. Nonstoichiometric phase with sillenite-type structure in the system  $\text{Bi}_2\text{O}_3\text{-P}_2\text{O}_5$ . *J. Solid State Chem.* 85: 76-82.
- Wignacourt, J.P., Drache, M., Conflant, P. and Boivin, J.C. 1991. New phases in  $\text{Bi}_2\text{O}_3\text{-BiPO}_4$  system. 2. Structure and electrical properties of sillenite type solid solution. *J. Chim. Phys.* 88: 1939-1949.
- Wignacourt, J.P., Drache, M., Conflant, P. and Boivin, J.C. 1991b. New phases in  $\text{Bi}_2\text{O}_3\text{-BiPO}_4$  system. 1. Description of phase diagram. *J. Chim. Phys. J. Chim. Phys.* 88: 1933-1938.